

# Exploring the effects of forcing quasi-biennial oscillations in a two-dimensional model

Philip A. Politowicz<sup>1</sup> and Matthew H. Hitchman

Department of Atmospheric and Oceanic Sciences, University of Wisconsin - Madison

**Abstract.** Analytic forcing of the stratospheric quasi-biennial oscillation (QBO) is introduced into a two-dimensional middle atmosphere model containing interactive radiation, dynamics, photochemistry and climatological aerosols. The “WISCAR” model integrates the temperature equation in time, but diagnoses the meridional stream function and zonal wind. An analytic forcing function for the QBO is derived from zonal wind observations and employed in three different ways: (1) as a “thermal nudge” in the temperature equation, or in the diagnostic meridional stream function equation as (2) additional heating or (3) equivalent wave driving. A different amplification factor for each method is required to achieve good agreement with the observed QBO in column ozone. This lends insight into the relationship among thermal perturbations, heating, and vertical motion. The vertical variation of QBO amplitude leads to a vertical dependence of the phase relationship among vertical motion, temperature, and zonal wind. Equatorial upward motions range from nearly zero to twice the time mean. Feedbacks in the model result in different extratropical responses for the two hemispheres and modulation of the equatorial semiannual oscillation. Chemical feedbacks and phase relationships are explored for the two ozone regimes: photochemical control above 30 km and advective control beneath. Confirming other studies, QBO vertical motions alter the distribution of odd nitrogen species above 30 km, which, together with the temperature dependence of reaction rates, combine to exert a strong control on ozone perturbations.

## 1. Introduction

The quasi-biennial oscillation (QBO) in the tropical stratosphere influences the global distributions of ozone [Angell and Korshover, 1964; Shah, 1967; Oltmans and London, 1982; Hasebe, 1980, 1983, 1994; Lait et al., 1989; Gruzdev and Moknov, 1992; Zerefos et al., 1992; Angell, 1993; Tung and Yang, 1994; Hamilton, 1995], stratospheric aerosol [Trepte and Hitchman, 1992; Hitchman et al., 1994], odd nitrogen and other constituents [Chipperfield et al., 1994] as well as winter hemisphere planetary wave activity and the ozone hole [O’Sullivan and Salby, 1990; Gray and Pyle, 1989; Gray and Dunkerton, 1990; Dunkerton and Baldwin, 1991]. The QBO may also be significant for tropospheric climate variations [e.g., van Loon and Labitzke, 1987; Xu, 1992; Yasunari, 1989; Zerefos et al., 1992; Gray et al., 1992].

The QBO is known to be driven by the absorption of vertically propagating equatorial waves [Lindzen and Holton, 1968; Holton and Lindzen, 1972; Plumb and

McEwan, 1978], yet modeling the QBO remains a challenge. Difficulties include generation of waves from convection in models, uncertainties in relevant wave types [J.W. Bergman and M. Salby, Equatorial wave activity calculated from fluctuations in observed convection, submitted to *J. Atmos. Sci.*, 1994], the complexity of balanced flows in the tropics [Stevens et al., 1990], the need for high vertical resolution due to “decoupling” in the vertical for tropical dynamics [Charney, 1963, 1969] and small vertical wavelengths [Takahashi and Boville, 1992], as well as uncertainties in the details of wave absorption. Other challenging quantitative aspects include the roles of cross-equatorial flow [Dunkerton, 1991] and photochemical feedbacks [Ling and London, 1986; Hasebe, 1994; Huang, 1996; Cordero et al., 1997].

Until recently, mechanistic two-dimensional (2D) models, which parameterize many of these processes, have been the most successful at simulating the QBO. Usually the effects of Kelvin and mixed Rossby-gravity waves are parameterized [Plumb, 1977; Dunkerton, 1981, 1985, 1991; Gray and Pyle, 1987; Takahashi and Holton, 1991; Chipperfield et al., 1994]. The resulting meridional circulation leads to extended meridional effects and alters the descent rate of QBO shear zones, as originally pointed out by Lindzen and Holton [1968]. Observations suggest that westerly shear zones descend more rapidly than easterly shear zones. Explanations for this

<sup>1</sup>Now at Space Science and Engineering Center, University of Wisconsin - Madison

“classical shear zone asymmetry” have also included differences in the effects of eastward and westward traveling waves and radiative feedback effects [Hasebe, 1994; Kinnersley and Pawson, 1995]. Because of the many unresolved issues, many modelers simply drag the flow toward the observed QBO winds [Chipperfield and Gray, 1992; Gray and Ruth, 1993; Chipperfield et al., 1990].

Three-dimensional (3D) model simulations [Dameris and Ebel, 1990; Holton and Austin, 1991; Koderer et al., 1991; Boville and Randel, 1992; Takahashi and Boville, 1992; Manzini and Hamilton, 1993] have obtained reasonable QBO zonal wind signals by using techniques such as specified Rossby-gravity, inertia-gravity, and Kelvin wave spectra and initializing QBO winds at a certain phase. Such studies explored the impact of various tropical waves on the stratospheric momentum budget, attempted to link these waves to tropospheric forcings, and found modulation of sudden stratospheric warmings by the QBO. Recently, Hess and O’Sullivan [1995] have simulated the extratropical ozone QBO using a 3D mechanistic model with an off-line transport code. Modeled and observed mixed Rossby-gravity waves still seem to be insufficient to drive the QBO easterly phase. Takahashi and Shiobara [1995] obtained a QBO-like oscillation in equatorial wind using a 1/5 sector 3D model derived from a prototype general circulation model and found that convectively generated gravity waves were important in driving the QBO in their model. It is becoming increasingly apparent that other gravity waves (as suggested originally by Lindzen and Holton [1968]), and perhaps meridionally propagating extratropical Rossby waves [Dunkerton, 1985; Kinnersley and Pawson, 1995], are needed to drive the QBO and that successful QBO simulations must account for the diabatic heating effects of the ozone QBO [Li et al., 1995].

This paper describes QBO simulations using a 2D middle atmospheric radiative-chemical-dynamical model (hereafter denoted the WISCAR model) that integrates temperature in time, but diagnoses zonal wind. Other models of the QBO calculate zonal winds by integrating the zonal momentum equation in time. The WISCAR model was designed for multiple decade integrations and has a time step of 15 days, rather than minutes. Recognizing the importance of the QBO to climate problems, we attempted to include the QBO while retaining this model architecture and hence the capability for long time integrations. This is interesting from a modeling and theoretical standpoint. It has been known since the late 1960s [Wallace, 1967a,b; Dickinson, 1969] that the QBO temperature perturbations must be maintained against radiative damping by meridional circulations. Thus, radiative damping should affect the thermal forcing required to achieve observed QBO zonal wind magnitudes.

Three QBO forcing parameterizations that produce good simulations of the QBO in dynamic fields and trace constituents will be described. Emphasis was

placed upon developing relatively simple, robust forcing parameterizations expressed as analytic functions which are readily differentiable and integrable in time and space. Observations of the zonal wind QBO are condensed into a compact analytic function in section 2. In section 3 the relevant governing equations of the WISCAR model and the three QBO forcing methods are described. Section 4 presents results from a control run with no QBO and salient results for the best QBO simulation (diabatic-forcing method), as determined by comparison with observations and previous benchmark simulations, as well as significantly different results for the wave-driving and thermal-nudge methods. Section 5 explores several specific modeling and theory issues raised by these experiments, including model resolution, coupling of tropical and extratropical middle atmospheric circulations, vertical dependence of the phase relationship among dynamical variables, and the changeover from dynamical to chemical control of the ozone QBO in the middle stratosphere. Section 6 contains conclusions and describes ongoing additional research. The interested reader is referred to [Huang, 1996] for applications of this parameterization to non-linear feedback studies in the WISCAR model.

## 2. Observations

Initial QBO wind observations were reported by Ver-  
yard and Ebdon [1961], Reed et al. [1961], [1965a,b], and Angell and Korshover [1962]. A useful survey of QBO observations and theoretical explanations was given by Wallace [1973]. QBO wind climatologies have been produced by Coy [1979], Hamilton [1984], Dunkerton and Delisi [1985], and Naujokat [1986]. These observations may be fit with a simple analytic functional form:

$$U_{QBO}(y, z, t) = U_o A(z) P(z, t) M(y). \quad (1)$$

The observed maximum QBO wind speed amplitude,  $U_o$ , is about 25 m/s near  $z_o = 28$  km. Significant QBO zonal wind amplitudes are contained approximately between 16 km and 40 km, so an amplitude envelope in altitude is specified:

$$A(z) = \cos \zeta, \quad \zeta = \frac{\pi (z - z_o)}{24 \text{ km}}, \quad (2)$$

with  $A = 0$  for  $z > 40$  km or  $z < 16$  km. The phase factor is chosen to represent the average observed QBO period of 27 months (821 days) and the zero wind line descent rate of 1 km/month:

$$P(z, t) = \cos \xi, \quad \xi = \frac{2 \pi t}{821 \text{ days}} + \frac{2 \pi (z - z_o)}{27 \text{ km}}. \quad (3)$$

One may include different descent rates for easterly and westerly shear. For this study equal descent rates were chosen to isolate other feedback effects more readily. From Wallace [1973], the observed QBO wind signal is seen to be roughly symmetric about the equator, decaying meridionally to  $(1/e)$  of its equatorial value near  $15^\circ$  latitude. This suggests a Gaussian meridional envelope

$$M(y) = e^{-(y/y^*)^2}, \quad (4)$$

where  $y^*$  is the meridional  $e$ -folding scale in meters, taken to correspond to 15° or 20°, as indicated below.

### 3. Experimental Design

#### 3.1. WISCAR Model

The WISCAR model is an interactive, zonally averaged middle atmospheric model described by *Brasseur et al.* [1990]. Photochemical calculations are done interactively, using the results of dynamic and radiation calculations. The radiation module is from the National Center for Atmospheric Research (NCAR) Community Climate Model version 2 (CCM2). The model domain is 85°S to 85°N latitude and 0 km to 85 km altitude, with resolutions of 5° and 1 km, respectively. This somewhat coarse meridional resolution leads to different amplitudes required for the three forcing methods. Interactive parameterizations of gravity and Rossby wave drag are included. The model is capable of simulating the effects a wide range of chemical and dynamical perturbations over many decades. The model code has been improved for the QBO simulations. The model tropopause heights, tropospheric zonal winds and temperatures now vary monthly according to the NCAR zonally averaged climatology of *Randel* [1987]. A more realistic distribution of vertical eddy diffusion coefficient has been introduced. Climatological stratospheric sulfate aerosol distributions calculated from a decade of Stratospheric Aerosol and Gas Experiment (SAGE) I and II, and Stratospheric Aerosol Measurement (SAM) II, satellite data [*Hitchman et al.*, 1994] affect the ozone chemistry. Initial model chemical constituent concentrations are based upon 1990 estimates. The seasonal variation of the tropospheric Hadley circulation is specified by an internal boundary condition on the meridional stream function at 15 km.

Model integration begins with calculation of the zonally averaged diabatic heating,  $Q$ , and net wave driving by Rossby and gravity waves:  $F = F_R + F_g$ . The parameterizations of  $F_g$  by *Lindzen* [1981] and  $F_R$  by *Hitchman and Brasseur* [1988] depend on model zonal winds. Then the zonal mean meridional mass stream function,  $\chi$ , is diagnosed to be compatible with the patterns of forcing by  $Q$  and  $F$ :

$$L^2 \chi = \cos \phi \left[ \frac{R}{H} \frac{\partial Q}{\partial y} + f \frac{\partial F}{\partial z} \right], \quad (5)$$

where " $L^2$ " is a spatial Laplacian operator defined by *Brasseur et al.* [1990]. This determines the transformed Eulerian mean, or residual, circulation ( $v^*$ ,  $w^*$ ). Given this circulation and net heating,  $Q$ , temperature is integrated with a 15 day time step:

$$\frac{\partial T}{\partial t} + v^* \frac{\partial T}{\partial y} + w^* \frac{\partial T}{\partial z} = Q, \quad (6)$$

where  $N_B$  is the buoyancy frequency. Zonal winds are then calculated by the thermal wind law,

$$\left( f + \frac{2u \tan \phi}{a} \right) \frac{\partial u}{\partial z} = -\frac{R}{H} \frac{\partial T}{\partial y}. \quad (7)$$

Equatorial zonal winds are obtained by averaging values at 5°N and 5°S.

#### 3.2. QBO Forcing Methods

Three different methods were tested for introducing a QBO into the WISCAR model. The "thermal-nudge" method adds a temperature tendency term to the right hand side of (6), while the "diabatic-forcing" and "wave-driving" methods add heating or equivalent wave driving to the rhs of (5). Note that the sign of the response is different for the thermal-nudge method than for the stream function forcing methods. For positive forcing, the thermal-nudge method yields a warm anomaly, which leads to anomalous radiative cooling and, hence, descent. For positive forcing of extra heating in (5), ascent results, yielding a cool anomaly. Thus positive forcing for the thermal-nudge method generates a westerly QBO pattern, while positive forcing for the diabatic-forcing method generates an easterly QBO pattern. In all cases, the model behaves energetically like the actual QBO: vertical motion and net heating correlate positively, and both correlate negatively with temperature tendency. This is consistent with the QBO's thermally indirect, wave-driven behavior.

**3.2.1. Thermal-nudge method.** Using the analytical expressions for zonal wind (1)-(4), differentiating in  $z$ , using the thermal wind law on an equatorial  $\beta$  plane,  $\beta y (\partial U / \partial z) = -(R/H) (\partial T / \partial y)$ , and integrating in  $y$ , one obtains

$$T_{QBO} = \frac{-U_o H \beta y^{*2}}{2R} M(y) \times \left[ \frac{\pi}{24 km} \sin \zeta \cos \xi + \frac{2\pi}{27 km} \cos \zeta \sin \xi \right], \quad (8)$$

where  $y^*$  is in meters,  $R=287 \text{ Jkg}^{-1}\text{K}^{-1}$ ,  $H=7000 \text{ m}$ ,  $a=6.37 \times 10^6 \text{ m}$ , and  $\beta = 2.29 \times 10^{-11} \text{ m}^{-1}\text{s}^{-1}$ . Observations indicate that the QBO temperature and inferred meridional circulation signatures reverse sign in the subtropics. An exponential meridional dependence for  $U_{QBO}$  does not capture this subtlety adequately, so an additional meridional nodal factor was used:

$$N(y) = \cos \left( \frac{\pi y}{2 y_n} \right), \quad (9)$$

where  $y_n$  is an adjustable effective meridional nodal scale length. Differentiating (8) in time and multiplying by (9), the QBO thermal nudge added to (6) is then

$$Q_{QBO} = \frac{-U_o H \beta y^{*2}}{2R} M(y) N(y) \frac{2\pi}{821 \text{ days}} \times \left[ \frac{2\pi}{27 \text{ km}} \cos \zeta \cos \xi - \frac{\pi}{24 \text{ km}} \sin \zeta \sin \xi \right]. \quad (10)$$

This leads to a temperature perturbation,  $\delta T$ , in (6) and altered net heating  $Q \propto -\delta T$  in the next time step. This both relaxes  $\delta T$  via (6) and changes the meridional circulation via (5). Thus, an initial  $Q_{QBO} > 0 \rightarrow Q \propto -\delta T < 0$  in the radiative code  $\rightarrow w < 0$  via (5), with a warm anomaly in westerly shear. In simulations using the thermal-nudge method, we chose initially  $U_o = 25$  m/s, with  $y^*$  and  $y_n$  corresponding to  $15^\circ$ . It was discovered empirically that reasonable QBO signals in zonal wind were obtained only after  $U_o$  was increased by a factor of 4. This is perhaps to be expected, since radiative damping reduces the effect of  $Q_{QBO}$ .

**3.2.2. Diabatic-forcing method.** In the diabatic-forcing method,  $Q_{QBO}$  from (10) is added to  $Q$  in (5), directly forcing the meridional circulation. In this method an initial  $Q_{QBO} > 0 \rightarrow w > 0$  in (5)  $\rightarrow \delta T < 0$  in (6)  $\rightarrow Q \propto -\delta T > 0$  in the radiative code, with a cool anomaly in easterly shear. It was found that  $U_o$  had to be increased from 25 m/s by a factor of 40 to achieve a satisfactory QBO. In this method a thermal perturbation must be maintained against damping by  $Q$ , which directly competes with  $Q_{QBO}$  in (5) for driving the requisite vertical motion. Although this augmentation of 40 arises from numerical issues, this method produces the best QBO signals in dynamical and chemical distributions. "Negative amplitude" simulations were also performed, with  $U_o$  multiplied by (-1), in order to assess the effects of initial forcing magnitude on model response; this is equivalent to shifting the phase by  $\pi$ .

**3.2.3. Wave-driving method.** In the wave-driving method, additional effective wave driving,  $F_{QBO}$ , was added to  $F$  in (5). One may consider  $F_{QBO}$  as a generalized forcing by Kelvin, mixed Rossby-gravity, inertia-gravity, and taller gravity waves.  $F_{QBO}$  is derived by equating the two forcing terms in (5), differentiating  $Q_{QBO}$  in  $y$ , integrating in altitude, and then multiplying by  $N(y)$ :

$$F_{QBO} = \frac{2\pi U_o}{821 \text{ days}} M(y) N(y) \cos \zeta \sin \xi. \quad (11)$$

Initially, the choices of  $U_o=25$  m/s and  $y^* = y_n$  corresponding to  $20^\circ$  were made. In this case,  $U_o$  had to be increased only by a factor of 1.75 to obtain satisfactory QBO signals in dynamic fields and trace constituents. This reduction in  $U_o$  relative to the diabatic-forcing method may be accounted for by model numerics.

## 4. Results

First, a short description of a control run with no QBO forcing will be presented. The diabatic-forcing

method generated the best overall QBO signatures, so its results will be described second and in greatest detail. Results from the wave-driving method were almost identical to those of the diabatic-forcing method, so they will not be shown. Thermal-nudge results are then presented, emphasizing departures from the diabatic-forcing method.

### 4.1. Control Run

A time-height section of equatorial zonal wind for the control run is shown in Figure 1. There is no detectable QBO in zonal wind. Time mean westerlies of  $\sim 10$  m/s occur in the upper troposphere, but the easterlies near 30 km are  $\sim 10$  m/s weaker than observations [Barnett and Corney, 1985]. The interaction between the model annual cycle and parameterized gravity waves generates a mild semi-annual oscillation (SAO) in the mesosphere. Although zonal wind seems to equilibrate within the first few time steps, some chemical constituents take up to a year to settle into regular behavior. After the first year, the control run column ozone signal (not shown) compares well with observations in the tropics, both in terms of timing and magnitude [e.g., Bowman and Kreuger, 1985]. This is also true in the extratropics, but minima are overpredicted and maxima are underpredicted by  $\sim 10$ -60 Dobson units (DU). These departures are modest for 2D model simulations [e.g., Newman, 1993].

To isolate differences due to the QBO forcing it is desirable to filter out the annual cycle, which is defined to exclude the initial two years of chemical equilibration. In presenting results in Figures 3-11, monthly means for years 3 through 10 were subtracted out. A Fourier filter was also applied, which eliminates timescales of less than 1 year in all figures except Figures 1, 2, and 9.

### 4.2. Diabatic-forcing Method

Figure 2 shows the equatorial time-height section of  $Q_{QBO}$  defined in (10). Heating maxima of  $\sim 1.3$  K/d occur at 28 km, with regular descent of  $Q_{QBO}$  heating anomalies confined between 16 and 45 km. Figures 3a, 4, and 5a show equatorial time-height sections for zonal wind, temperature, and vertical wind. As argued qualitatively in section 3.2.2., initial positive heating near 28 km leads to rising cool air in easterly shear. Initial negative heating (not shown) leads to sinking warm air in westerly shear. Zonal wind maxima near 30 km are  $\sim 22$  m/s, reasonably close to observations [Naujokat, 1986]. Near 30 km, westerly and easterly wind signatures decay significantly by  $\pm 30^\circ$  latitude from their respective maxima (Figure 3b), also in accord with observations [Wallace, 1973]. A descent rate asymmetry was not included in the forcing equation. However, simulations without an imposed meridional nodal factor displayed westerly shear predominance in the lower stratosphere (not shown).

The QBO temperature signal maximizes at  $\sim 3$  K near 28 km and is largely confined below 45 km (Figure 4), in accord with observations and other simulations



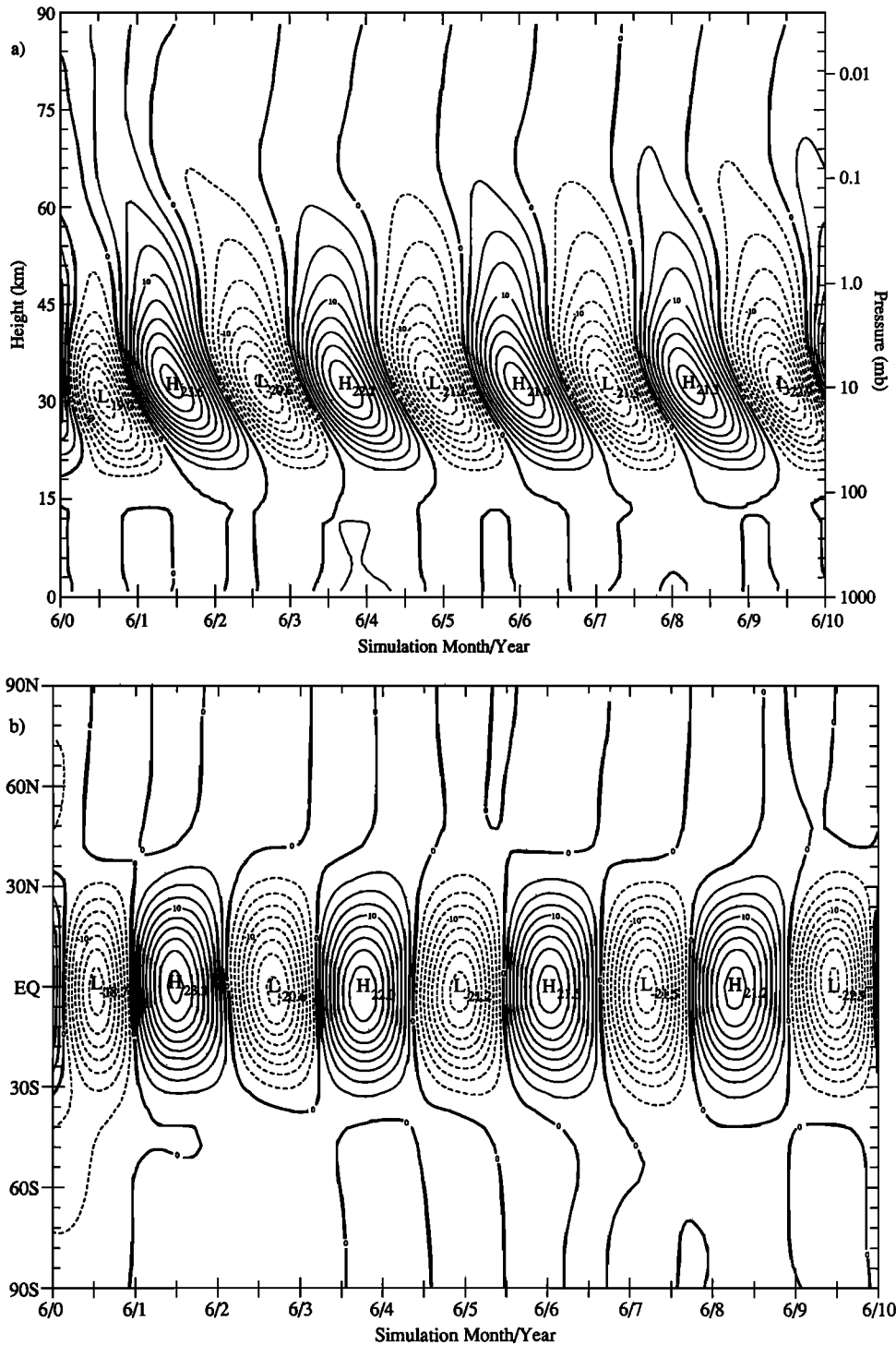


**Figure 3.** QBO zonal wind signal for the diabatic-forcing method, after removal of monthly means and filtering to remove all signal oscillations with period less than 360 days: (a) equatorial time-altitude section, (b) time-latitude section at 30 km altitude. Contour interval is 2.5 m/s.

and 5a). QBO vertical motions peak at  $\sim \pm 0.3$  mm/s ( $\sim 0.8$  km/month) near 30 km. Total vertical motion in the lower stratosphere ranges from  $\sim 0.5$  mm/s during QBO easterlies to  $\sim 0.01$  mm/s during QBO westerlies. A significant signal in vertical motion is seen well into the mesosphere. Mesospheric vertical motions are in phase with the sign of  $Q_{QBO}$  near 35 km.

The subtropical return branches of the meridional circulation are highlighted in Figure 5b, which shows a time-latitude section of  $w$  at 30 km. Subtropical anomalies are reversed in sign, being about half as strong as coincident tropical maxima. This meridional circulation has important implications for column ozone. Since the source for ozone maximizes near 30 km, ascent within

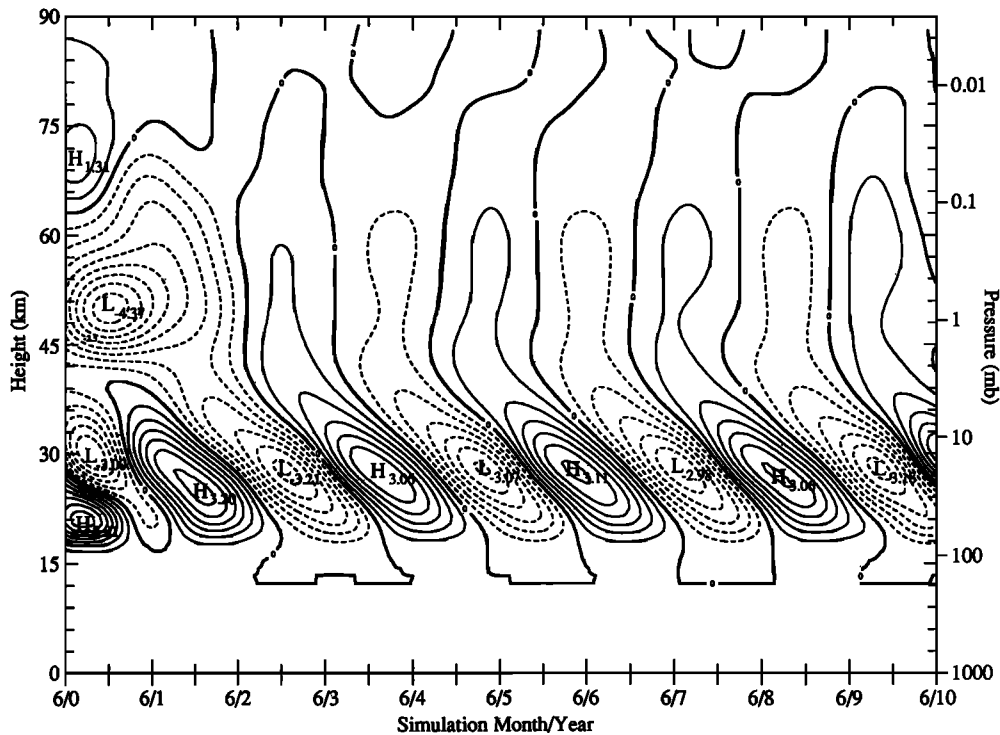


**Figure 4.** Equatorial time-altitude section of QBO temperature signal for the diabatic-forcing method, after removal of monthly means and filtering; contour interval is 0.5 K.

QBO westward shear and poleward advection near the westward maximum diminishes tropical column ozone, while column ozone is enhanced in the subsiding subtropical return circulation. This is the essence of the

phase reversal for column ozone across the subtropics near  $\pm 15^\circ$  shown by *Reed [1965]*, *Shah [1967]*, *Angell and Korshover [1973]*, *Ohmans and London [1982]*, *Hasebe [1983]*, *Zawodny and McCormick [1991]*, *Tung*

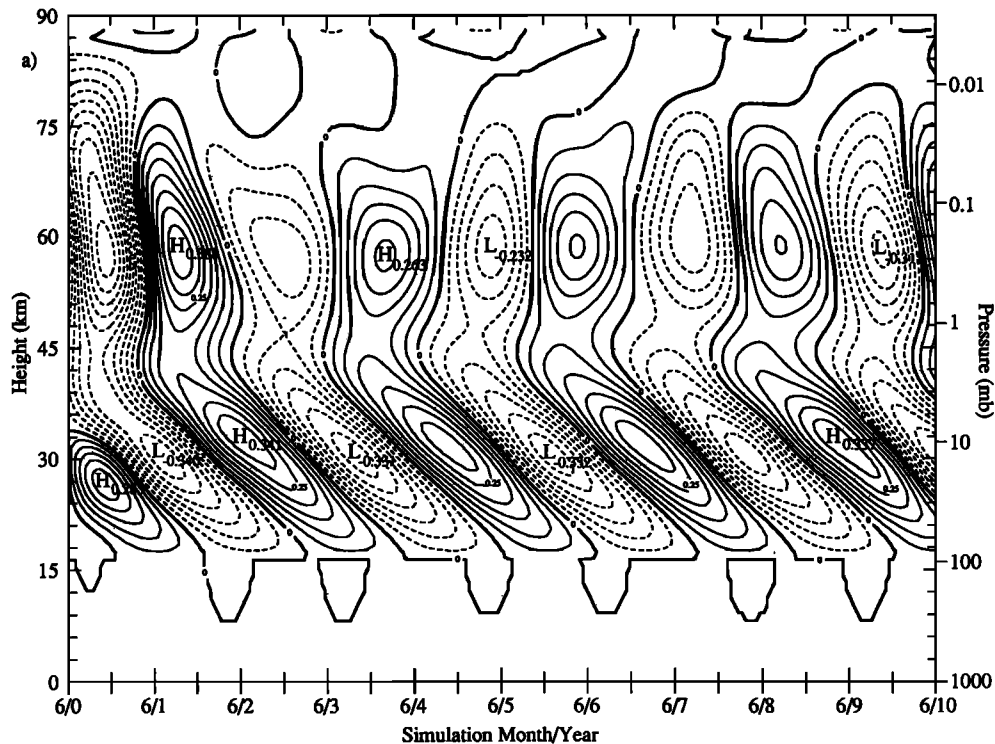


**Figure 5.** As in Figure 3, except of vertical wind, with contour interval of 0.05 mm/s.



during QBO easterly shear. After the first few years a QBO in tropical column ozone emerges, with amplitudes of  $\sim 10$  DU, similar to observations. Tropical column ozone maxima occur when eastward shear dominates below 30 km, while ozone minima occur when westward shear dominates (cf. Figure 3a). A phase reversal between tropical and subtropical anomalies occurs at about  $\pm 15^\circ$ , a result which is sensitive to the choice of  $y_n$ . Similar behavior has been obtained in the simulations of *Gray and Dunkerton [1990]*, *Chipperfield and Gray [1992]*, *Gray and Ruth [1993]*, and *Tung and Yang [1994a]*.

Extratropical anomalies are slightly greater ( $\sim 14$  DU) than in the tropics, with intermittent annual modulation. In middle and polar latitudes, column ozone varies with a periodicity of  $\sim 20$  months, nearly the beat frequency between the QBO and the annual cycle [*Hamilton, 1995*]. An annual modulation of the ozone QBO should occur due to transport by extratropical planetary Rossby waves [*Gray and Pyle, 1989*]. *Tung and Yang [1994b]* provide an interesting discussion of dynamical mechanisms regarding the extratropical QBO in column ozone. In the WISCAR model, transport by extratropical planetary waves depends on model winds, and the tropopause wave activity is specified to be weaker in the southern winter. The rudiments of this wave - mean flow feedback effect on extratropical column ozone operate in this model. Southern hemisphere maxima occur in the midlatitudes, while northern hemisphere maxima tend to include the highest latitudes.

Figure 7 shows an equatorial time-height section of the ozone QBO signal. The ozone signal maximizes around 28 km, with amplitudes reaching 1 ppmv, or  $\sim 10\%$  of the long-term average. Below  $\sim 32$  km the ozone anomaly is anticorrelated with vertical motion,

being high in subsiding QBO westerly shear. A distinct transition occurs near 32 km, from advective control below to photochemical control above. In the photochemical regime, upward motion coinciding with lower temperatures reduces ozone destruction by odd nitrogen species,  $\text{NO}_y$ , and promote its formation. We find that the QBO affects ozone destruction by  $\text{NO}_y$  both by modulating the advection of  $\text{NO}_y$  and by modulating the temperature-dependent reaction rates.

Figure 8a shows an equatorial time-height section of the QBO signal in  $\text{NO}_y = \text{NO} + \text{NO}_2 + \text{NO}_3 + \text{HO}_2\text{NO}_2 + \text{ClONO}_2 + \text{HNO}_3 + 2\text{N}_2\text{O}_5$ .  $\text{NO}_y$  is primarily responsible for ozone destruction in the upper stratosphere, with  $\text{NO}_y$  concentrations peaking near 40 km. Unlike ozone, the  $\text{NO}_y$  signal is very weak below 25 km. Maximum anomalies of  $\sim 1.5$  ppbv occur near 32 km. By comparing with Figure 5a it is apparent that QBO ascent decreases  $\text{NO}_y$  and QBO descent increases  $\text{NO}_y$ . Thus in the photochemical control region during QBO easterly shear, reduced  $\text{NO}_y$  and lower temperatures coincide with higher ozone, while enhanced  $\text{NO}_y$  and higher temperatures coincide with lower ozone (Figure 7).

Figure 8b shows that the  $\text{NO}_y$  signal extends well into middle latitudes. Tropical and extratropical responses are consistently out of phase, yet the latitudinal phase relationship is somewhat different than for vertical motion (cf. Figure 5b). The magnitude of the subtropical  $\text{NO}_y$  signal is  $\sim 75\%$  of the tropical signal. This  $\text{NO}_y$  signal is similar to that of *Gray and Dunkerton [1990]*, but the tropical signal is stronger, in accordance with the stronger QBO meridional circulation. *Chipperfield and Gray [1992]* and *Chipperfield et al. [1994]* found that  $\text{NO}_y$  modulation dominates the ozone QBO signal changes above 28 km and that  $\text{NO}_y$  QBO signals can

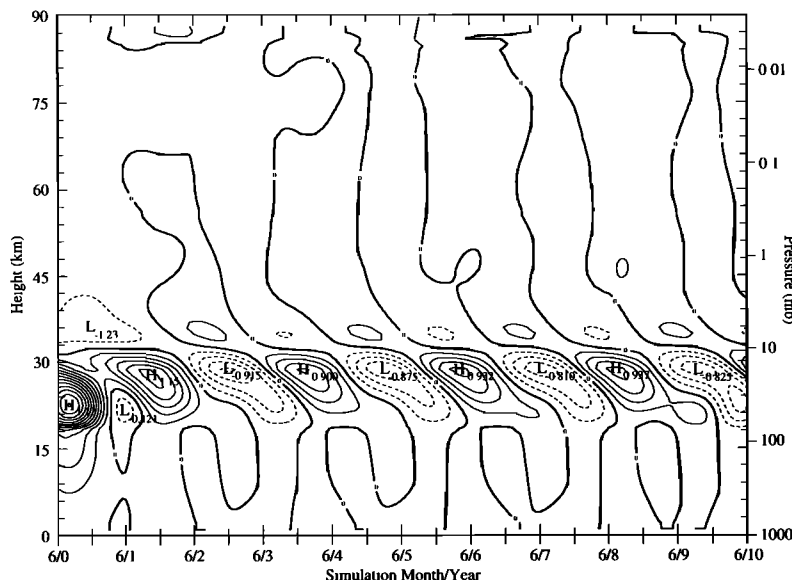


Figure 7. As in Figure 3a, except of ozone mixing ratio, with contour interval of 0.12 ppmv.



stream function forcing methods are striking. Although the range in thermally driven QBO zonal wind signal (not shown) is similar to that of the other two methods, the temperature range is  $\sim 25\%$  greater in the thermal-nudge method, yet is more confined to the forcing region. Due to this confinement, the QBO in ozone and  $\text{NO}_y$  are weaker everywhere (not shown).

## 5. Discussion

Several issues raised by the model results are now addressed: influences of model numerics on simulated QBO signals, dynamical feedbacks, signal amplitudes and phase relationships, and the effect of the QBO on ozone destruction by various chemical families.

### 5.1. Model Numerics

In the thermal-nudge, diabatic-forcing, and wave-driving methods, the forcing amplitude was multiplied by a factor of 4, 40, and 1.75, respectively. In focusing on the diabatic-forcing method, it is possible that the factor of 40 might reflect a decoupling between the energy reservoir associated with the thermal perturbation ( $\overline{PE}$ ) and that of the zonal mean zonal wind ( $\overline{KE}$ ). Indeed, *Plumb and Bell* [1982a] estimated the ratio of  $\overline{KE}/\overline{PE}$  to be  $\sim 40$  in the tropical stratosphere. The concern is that any model which does not explicitly integrate an equation for the zonal mean meridional motion cannot account for this energetic coupling. Yet the temperature and zonal flow are exactly related through the thermal wind law, so this coupling is effectively instantaneous. An alternative explanation lies in the coarse meridional resolution of the QBO forcing.

For all forcing methods, the QBO zonal wind signal is very sensitive to the value of the meridional nodal position  $y_n$ . In the diabatic-forcing simulation,  $y_n = 10^\circ$  eliminated the QBO for any forcing amplitude. With a model meridional resolution  $\delta y = 5^\circ$  and with  $y_n = 10^\circ$ , equatorial forcing is nonzero at only three tropical points. On the other hand,  $y_n = 20^\circ$  and  $25^\circ$  gave equatorial QBO zonal wind amplitude maxima of 50 m/s and 80 m/s, respectively. In the "best" simulation using the diabatic-forcing method with  $y_n = 15^\circ$ , the meridional stream function forcing is given by a finite difference representation of  $\partial Q/\partial y$ , which maximizes at  $\pm 10^\circ$ . In the wave-driving method, the meridional stream function responds to  $\partial F/\partial z$ , which is a vertical finite difference in altitude, at a resolution of 1 km, of a function which contains an analytic representation of  $\partial Q/\partial y$ . Moreover,  $y_n$  was taken to be larger for the wave-driving simulation. This resulted in a much smaller multiplication factor in the wave-driving simulation. The value of  $n_y$  also determines whether or not a shear zone asymmetry forms. Further study of the effects of  $\delta y$  and  $n_y$  is warranted. A model version with  $2.5^\circ$  resolution is currently under development. Despite this uncertainty, a result common to all methods is that when one forces a QBO thermally,

augmentation is required to offset radiative damping of forced thermal anomalies intended to generate a zonal wind QBO.

### 5.2. Dynamical Feedbacks

QBO signals defined as a deviation from the control run fields are not shown in this work. However, they do show some interesting behavior. Many QBO signals so defined possess meridional asymmetry; chemical signals usually are more intense and extend farther into the northern hemisphere. This meridional asymmetry of QBO signals is due to a combination of several factors: hemispheric asymmetries in Rossby wave activity, the specified annual cycle in the Brewer-Dobson circulation, insolation intensity, chemical sources, and nonlinear gravity wave feedback in the model. In the extratropics, annual modulation of QBO trace constituent signals is due to modulation of Rossby wave transport. During QBO easterlies, the winter hemisphere zero wind line is closer to the pole, focusing Rossby wave activity and eddy transport poleward. But during the westerly phase, Rossby waves propagate into the (sub)tropics, thus reducing wave activity and poleward eddy transport. There is also a hemispheric asymmetry in stratospheric Rossby wave activity, favoring the northern hemisphere, which is explicitly included in the model. Stratospheric Rossby wave activity is therefore relatively smaller in the southern winter.

### 5.3. QBO Amplitude and Phase Relationships

The evolution of equatorial zonal wind, temperature, and ozone at 25 and 35 km are shown in Figures 9a and 9b. Below 30 km, ozone is controlled advectively and is highly correlated with temperature, since descent brings down higher values of ozone and entropy. Above 32 km, ozone is controlled photochemically, and is highly anticorrelated with temperature. This is consistent with SAGE data [*Hasebe*, 1994]. *Hasebe* suggested that the feedback due to ozone solar heating would enhance QBO temperature anomalies in the advective regime. Subsiding warm ozone-rich air would absorb more sunlight, helping to maintain the warm anomaly, while ascending cool ozone-poor air would absorb less sunlight, helping to maintain the cool anomaly. Qualitatively, this effect is also occurring in the WISCAR model, but we defer a more detailed interpretation until further quantitative analysis. Here it is of interest to focus on the phase shift between temperature and wind with altitude.

Near 25 km (Figure 9a), temperature leads zonal wind by about a  $1/4$  cycle, while at 35 km temperature leads by nearly a  $1/2$  cycle. The latter situation is a distinct departure from canonical views of the QBO. Yet it is to be expected since there are vertical and meridional amplitude envelopes imposed on the vertical sinusoid via (2) and (4), and zonal wind is a vertical integral of meridional temperature gradients in layers below, as in (7). Thus temperatures near 28 km contribute most

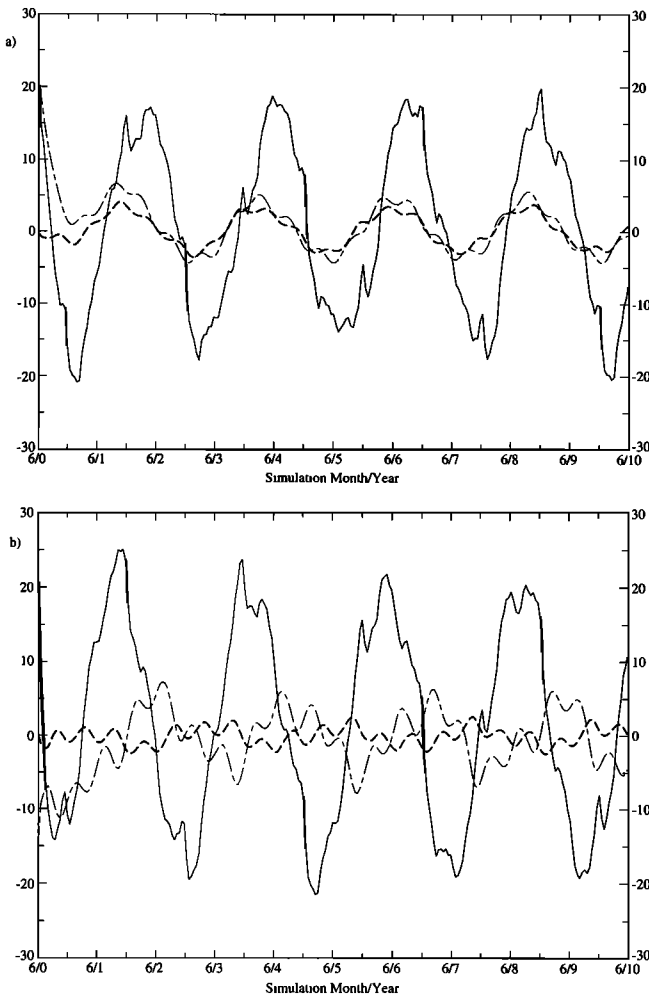


**Figure 9.** Evolution of QBO in zonal wind (solid, m/s), temperature (dashed, K), and ozone (short/long dashed, ppmv times 10) over the equator at (a) 25 km and (b) 35 km.

to zonal winds above that layer. When a warm maximum occurs near 28 km, the smaller cold maximum aloft cannot close off the QBO westerly jet. The zonal wind solution is "taller" than the temperature solution (compare Figures 3a and 4), with a tendency to become out of phase at higher altitudes.

This is seen more clearly in Figure 10, which shows amplitudes and phases for QBO  $u$ ,  $T$ ,  $w$ ,  $O_3$ , and  $NO_y$  anomalies over the equator. Below 32 km, the zonal wind signal displays a vertical envelope structure similar to  $A(z)$  in (2). However, the zonal wind signal deviates above this level, extending well above the QBO forcing regime. The vertical wind field actually reaches a secondary maximum around 60 km (Figure 5a), and the vertical advection forces QBO signals in ozone and  $NO_y$  to extend well above 42 km. The minimum in ozone signal amplitude near 31 km marks the transition from advective to photochemical control. The upward extension of a significant QBO response is due to nonlinearities in the model response to vertically confined thermal forcing.

The phase lag of  $T$ ,  $w$ ,  $O_3$ , and  $NO_y$  with respect to zonal wind shows a significant vertical dependence (Figure 10b). Below  $\sim 28$  km temperature leads zonal wind by  $\sim 3$ –4 months, but this lead becomes larger with altitude, with temperature becoming nearly anticorrelated with zonal wind by 45 km. Vertical motion tends to stay anticorrelated with temperature at all levels, meaning that near 20 km  $u$  and  $w$  are out of phase, but near 40 km they are in phase. This shift in phase between  $u$  and  $T$  or  $w$  is quite striking and invites further study. Below 30 km, ozone is out of phase with vertical velocity. Beyond the transition zone, above 32 km, ozone is out of phase with  $NO_y$ , a relationship which is explored further in the next section. The altitude dependence of the  $u$ – $w$  relationship is important to keep in mind when interpreting ozone feedbacks in terms of zonal wind shear zones. Below 30 km, ozone maxima precede zonal wind

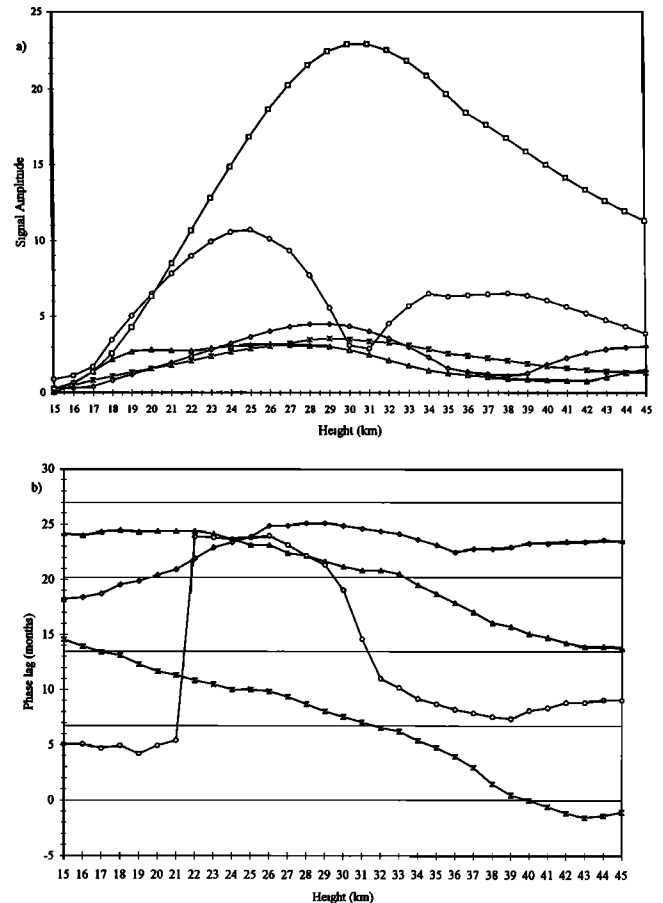


**Figure 10.** (a) Amplitude and (b) phase lag in months relative to zonal wind for the diabatic-forcing method, after subtraction of monthly means and Fourier filtering to remove all signal oscillations with period less than 360 days: zonal wind (squares, m/s), ozone (circles, ppmv times 10),  $NO_y$  (diamonds, ppbv), vertical motion (asterisks,  $10^{-4}$  m/s), and temperature (triangles, K). In Figure 10b, thin horizontal lines mark phase lags of: 0 cycle (0 months), 1/4 cycle (6.75 months), 1/2 cycle (13.5 months), 3/4 cycle (20.25 months), and 1 cycle (27 months).

maxima by 3-4 months, while above 32 km ozone maxima lag zonal wind maxima by 7-8 months.

#### 5.4. Ozone Destruction in the QBO

The ozone concentration QBO displays a rich vertical structure (Figure 7), in part due to the vertical variation of ozone destruction by chemical families. Figures 11a-11d show equatorial time-altitude sections of the QBO ozone destruction signal in the diabatic-forcing method simulation for the  $\text{NO}_y$ , (Figure 11a),  $\text{HO}_x = \text{H} + \text{HO}_2$  (Figure 11b),  $\text{O}_x = \text{O} + \text{O}_3$  (Figure 11c), and  $\text{Cl}_x = \text{ClO} + \text{HCl} + \text{Cl} + \text{HOCl} + \text{OCIO} + 2 \text{Cl}_2\text{O}_2 + \text{ClONO}_2$  (Figure 11d) families. Values contoured in Figure 11 are the QBO departure of ozone destruction for a given family, divided by the total ozone destruction for all families. In the control run, the net destruction

of ozone is a maximum at 42 km, and ozone destruction is dominated by  $\text{HO}_x$  between 15 km and 20 km,  $\text{Cl}_x$  between 20 km and 27 km, as well as above 45 km, and  $\text{NO}_y$  between 30 km and 45 km;  $\text{O}_x$  destruction is competitive, but not dominant, at around 30 km and 50 km.

The strongest signal in QBO destruction of ozone by  $\text{NO}_y$  at the equator (Figure 11a) occurs primarily between 28 km and 40 km, and ranges between +5% and -5%, not including the initial equilibration period. In this region, control run  $\text{NO}_y$  destruction of ozone increases upward from near 20% at 30 km to 50% at 40 km, with slight annual variations. Maxima (minima) in QBO signals in  $\text{NO}_y$  destruction of ozone are coincident with ozone signal minima (maxima) around 35 km. But  $\text{NO}_y$  destruction signal maxima extend down

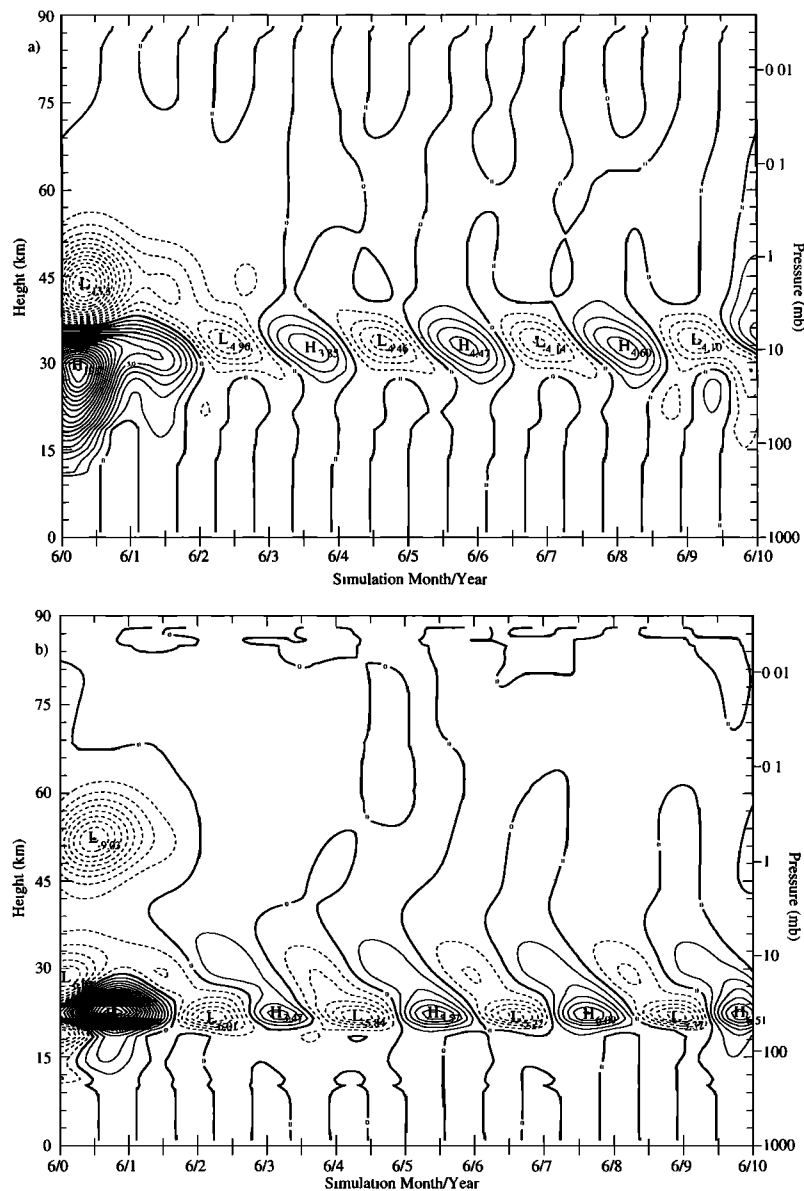


**Figure 11.** Percent QBO anomaly of ozone loss rate due to a given chemical family, relative to total ozone loss from all families for (a)  $\text{NO}_y$ , (b)  $\text{HO}_x$ , (c)  $\text{O}_x$ , and (d)  $\text{Cl}_x$ . The contour interval is 1%, except for 0.5% in Figure 11c.

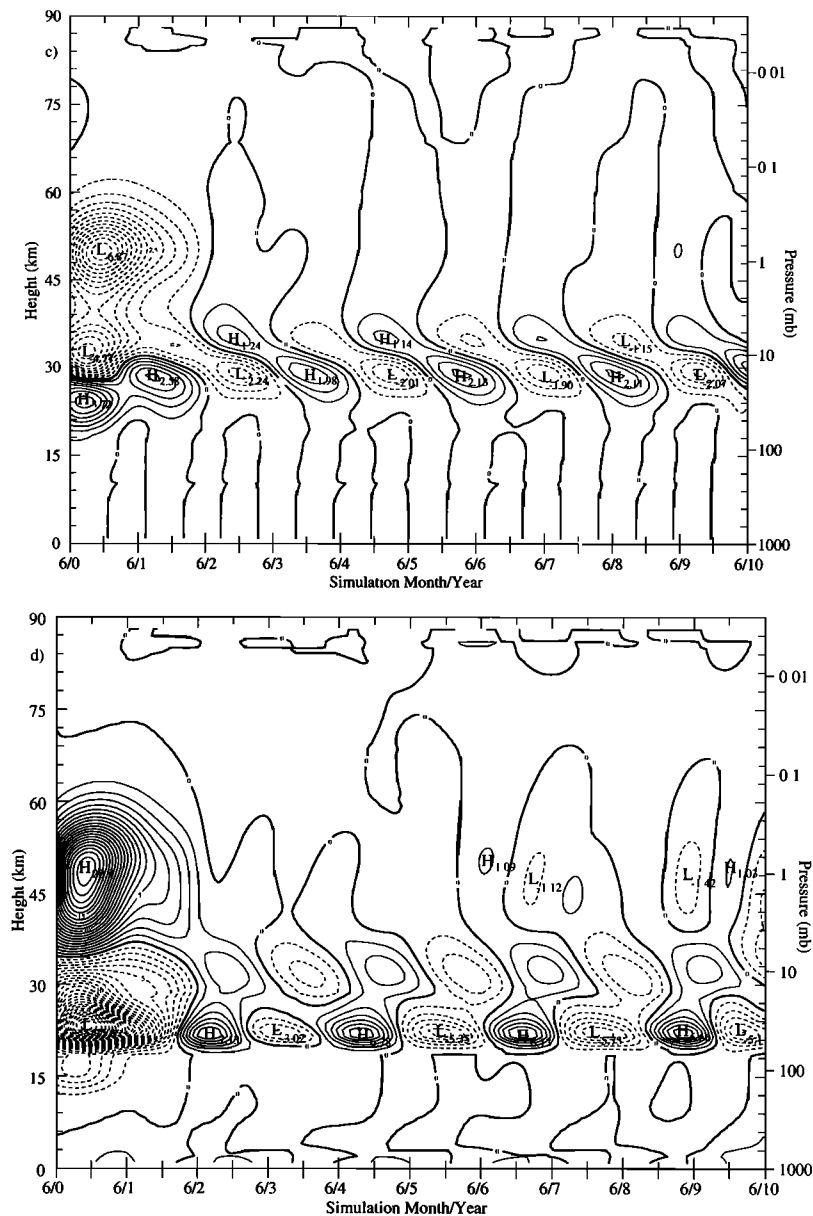


Figure 11. (continued)

to 25 km, contributing to the dephasing of ozone, zonal wind, and temperature signals. A latitude-time section of QBO  $\text{NO}_y$  destruction of ozone (not shown) appears almost identical to that of  $\text{NO}_y$  itself, with significant extensions into middle latitudes.

The strongest simulated QBO signal in ozone destruction by  $\text{HO}_x$  outside of the initial model equilibration (Figure 11b) ranges between +6% and -6% and is centered near 22 km. Control run  $\text{HO}_x$  destruction of ozone decreases upward from near 90% at 15 km to 45% at 22 km, with slight annual variations. The  $\text{HO}_x$  ozone destruction signal is antiphased with respect to the ozone signal in the advective control regime. However, the two signals are in phase in the photochemical control regime. The  $\text{O}_x$  ozone destruction signal (Figure 11c) behaves similarly. Net upward motion at 21 km will en-

hance  $\text{HO}_x$ , decrease  $\text{ClO}_x$  and decrease  $\text{O}_3$ . At 25 km, extratropical signal maxima (minima) in QBO  $\text{HO}_x$  destruction of ozone are well correlated with ozone signal minima (maxima). The  $\text{Cl}_x$  ozone destruction signal (Figure 11d) is strongest near the bottom of the QBO forcing regime and is antiphased with respect to the ozone signal. However, there is a secondary amplitude maximum centered at the transition level between advective and photochemical control.

The QBO produces signals in chemical constituents also through variations in the distribution of sulfate aerosol and development of PSC, via heterogeneous processes. Further model simulations, using stratospheric aerosol distributions derived for distinct phases of the QBO [Hitchman *et al.*, 1994] are addressing the aerosol QBO signal and its chemical effects.

## 6. Conclusions

The present work shows the methods and results of introducing simple, analytic function parameterizations of various QBO forcings into a 2D middle atmospheric model in which the thermodynamic equation, not the zonal momentum equation, is integrated in time. Adopting a pragmatic approach, the model's governing equations permitted three forcing methods, each derived from a single idealized functional representation in space and time of QBO perturbation zonal winds. One forcing method stems from a simple thermal wind relationship: a QBO thermal perturbation is added at each time step, which in turn generates a distinct QBO wind perturbation. The two other approaches proceed through the wave driving and diabatic heating forcing terms in the meridional stream function equation.

Of the three forcing methods, the simulation using the diabatic-forcing method gave the best results, as compared with observations and theoretical results. The wave-driving method simulation was almost as successful as the diabatic-forcing method simulation, but the trace species signals and meridional extent of the dynamic signals were weaker. The thermal-nudge simulation produced generally poorer QBO signals overall, particularly in the trace species signatures. In this model, the tropically forced QBO generates a global meridional circulation, creating substantial extratropical signals by interacting with extratropical planetary wave-driven circulations [Dickinson, 1968; Plumb and Bell, 1982b; Garcia and Solomon, 1987]. QBO signals in temperature, meridional circulation, diabatic heating and cooling reach well into middle latitudes, and the QBO signals in the trace species, such as ozone and  $\text{NO}_y$ , at some vertical levels are strong into middle latitudes. The results indicate that the QBO vertical motion signal in the lower stratosphere is comparable to, but never reverses, the Brewer-Dobson circulation's persistent upward motion.

This work suggests several areas for future model improvement. Successful QBO simulations with a prescribed analytic basic state variation now allow exploration of a more interactive parameterization using linear theory for Kelvin, mixed Rossby-gravity and inertia-gravity waves. This should allow a shear zone asymmetry and variable QBO period to develop. The conditions under which shear zone descent asymmetry develops in the model are important, since empirical orthogonal function (EOF) analysis by Fraedrich *et al.* [1993] shows rather uniform descent, while a similar EOF analysis by Wallace *et al.* [1994] argues that the strong phase progression of the zonal wind QBO dominates any annual cycle contribution. Yao [1994] suggests that the apparently slow descent of QBO easterlies is due primarily to incomplete removal of the local annual cycle. Further studies will compare the relative influences of this QBO dynamical parameterization and climatological distributions of aerosol surface area compiled for the two phases of the QBO.

**Acknowledgments.** We thank Chip Trepte and Megan McKay for their work on the WISCAR model. We thank Fumio Hasebe, Theresa Y.-W. Huang, and an anonymous reviewer for their useful suggestions. The National Aeronautics and Space Administration supported this research under grants NAGW-2943 and NAG-1-1403. We also acknowledge use of computing resources at the National Center for Atmospheric Research, which is supported by the National Science Foundation.

## References

- Andrews, D. G., J. R. Holton, and C. B. Leovy, *Middle Atmosphere Dynamics*, 489 pp., Academic, San Diego, Calif., 1987.
- Angell, J. K., Reexamination of the relationship between the depth of the Antarctic ozone hole and equatorial QBO and SST, 1962-1992, *Geophys. Res. Lett.*, **20**, 1559-1562, 1993.
- Angell, J. K., and J. Korshover, The biennial wind and temperature oscillations of the equatorial stratosphere and their possible extension to higher latitudes, *Mon. Weather Rev.*, **90**, 127-132, 1962.
- Angell, J. K., and J. Korshover, Quasi-biennial variations in temperature, total ozone and tropopause height, *J. Atmos. Sci.*, **21**, 479-492, 1964.
- Barnett, J. J., and M. Corney, Middle atmosphere reference model derived from satellite data, in *MAP Handbook 16*, SCOSTEP Secretariat, Urbana, Ill., 1985.
- Boville, B. A., and W. J. Randel, Equatorial waves in a stratospheric GCM: Effects of vertical resolution, *J. Atmos. Sci.*, **49**, 785-801, 1992.
- Bowman, K. P., and A. J. Krueger, A global climatology of total ozone from the Nimbus 7 total ozone mapping spectrometer, *J. Geophys. Res.*, **90**, 7967-7976, 1985.
- Brasseur, G., M. H. Hitchman, S. Walters, M. Dymek, E. Falise, and M. Pirre, An interactive chemical dynamical radiative two-dimensional model of the middle atmosphere, *J. Geophys. Res.*, **95**, 5639-5655, 1990.
- Butchart, N., and J. Austin, On the relationship between the quasi-biennial oscillation, total chlorine and the severity of the Antarctic ozone hole, *Q. J. R. Meteorol. Soc.*, **122**, 183-217, 1996.
- Charney, J. G., A note on large-scale motions in the tropics, *J. Atmos. Sci.*, **20**, 607-609, 1963.
- Charney, J. G., A further note on large-scale motions in the tropics, *J. Atmos. Sci.*, **26**, 182-185, 1969.
- Chipperfield, M. P., and L. J. Gray, Two-dimensional model studies of the interannual variability of trace gases in the middle atmosphere, *J. Geophys. Res.*, **97**, 5963-5980, 1992.
- Chipperfield, M. P., L. J. Gray, J. S. Kinnersley, and J. Zawodny, A two-dimensional model study of the QBO signal in SAGE II  $\text{NO}_2$  and  $\text{O}_3$ , *Geophys. Res. Lett.*, **21**, 589-592, 1994.
- Cordero, E. C., T. R. Nathan, and R. S. Echols, An analytical study of the effects of ozone heating on the QBO, *J. Atmos. Sci.*, in press, 1997.
- Coy, L., An unusually large westerly amplitude of the quasi-biennial oscillation, *J. Atmos. Sci.*, **36**, 174-176, 1979. (Corrigendum, *J. Atmos. Sci.*, **37**, 9 12-913, 1980).
- Dameris, M., and A. Ebel, The quasi-biennial oscillation and major stratospheric warmings: A three-dimensional model study, *Ann. Geophys.*, **8**, 79-86, 1990.

- Dickinson, R. E., On the excitation and propagation of zonal winds in an atmosphere with Newtonian cooling, *J. Atmos. Sci.*, *25*, 269-279, 1968.
- Dickinson, R. E., Theory of planetary wave-zonal flow interaction, *J. Atmos. Sci.*, *26*, 73-81, 1969.
- Dunkerton, T. J., On the mean meridional mass motions of the stratosphere and mesosphere, *J. Atmos. Sci.*, *35*, 2325-2333, 1978.
- Dunkerton, T. J., Wave transience in a compressible atmosphere, II, Transient equatorial waves in the quasi-biennial oscillation, *J. Atmos. Sci.*, *38*, 298-307, 1981.
- Dunkerton, T. J., A two-dimensional model of the quasi-biennial oscillation, *J. Atmos. Sci.*, *42*, 1151-1160, 1985.
- Dunkerton, T. J., Nonlinear propagation of zonal winds in an atmosphere with Newtonian cooling and equatorial wavelike driving, *J. Atmos. Sci.*, *48*, 236-263, 1991.
- Dunkerton, T. J., and M. P. Baldwin, Quasi-biennial modulation of planetary-wave fluxes in the Northern hemisphere winter, *J. Atmos. Sci.*, *48*, 1043-1061, 1991.
- Dunkerton, T. J., and D. P. Delisi, Climatology of the equatorial lower stratosphere, *J. Atmos. Sci.*, *42*, 376-396, 1985.
- Fraedrich, K., S. Pawson, and R. Wang, An EOF analysis of the vertical-time delay structure of the quasi-biennial oscillation, *J. Atmos. Sci.*, *50*, 3357-3365, 1993.
- Garcia, R. R., and S. Solomon, A possible relationship between interannual variability in Antarctic ozone and the quasi-biennial oscillation, *Geophys. Res. Lett.*, *14*, 848-851, 1987.
- Gray, L. J., and T. J. Dunkerton, The role of the seasonal cycle in the quasi-biennial oscillation of ozone, *J. Atmos. Sci.*, *47*, 2429-2451, 1990.
- Gray, L. J., and J. A. Pyle, Two-dimensional model studies of equatorial dynamics and tracer simulations, *Q. J. R. Meteorol. Soc.*, *113*, 635-651, 1987.
- Gray, L. J., and J. A. Pyle, A two-dimensional model study of the quasi-biennial oscillation of ozone, *J. Atmos. Sci.*, *46*, 203-220, 1989.
- Gray, L. J., and S. Ruth, The modeled latitudinal distribution of the ozone quasi-biennial oscillation using observed equatorial winds, *J. Atmos. Sci.*, *50*, 1033-1046, 1993.
- Gray, W. M., C. W. Landsea, P. W. Mielke, and K. J. Berry, Predicting Atlantic seasonal hurricane activity 6-11 months in advance, *Weather Forecast.*, *7*, 440-455, 1992.
- Gruzdev, A. N., and I. I. Mokhov, Quasi-biennial oscillation in global total ozone field as derived from ground-based observations, *Izv. Atmos. Ocean. Phys.*, *28*, 475-486, 1992.
- Hamilton, K., Mean wind evolution through the quasi-biennial cycle in the tropical lower stratosphere, *J. Atmos. Sci.*, *41*, 2113-2125, 1984.
- Hamilton, K., Comment on "Global QBO in circulation and ozone, I, Reexamination of observational evidence", *J. Atmos. Sci.*, *52*, 1834-1838, 1995.
- Hasebe, F., A global analysis of the fluctuation of total ozone, II, Non-stationary annual oscillation, quasi-biennial oscillation, and long-term variations in ozone, *J. Meteorol. Sci. Jpn.*, *58*, 104-117, 1980.
- Hasebe, F., Interannual variations in global total ozone revealed from Nimbus 4 BUUV and ground-based observations, *J. Geophys. Res.*, *88*, 6819-6834, 1983.
- Hasebe, F., Quasi-biennial oscillations of ozone and diabatic circulation in the equatorial stratosphere, *J. Atmos. Sci.*, *51*, 729-745, 1994.
- Hess, P. G., and D. O'Sullivan, A three-dimensional modeling study of the extratropical quasi-biennial oscillation in ozone, *J. Atmos. Sci.*, *52*, 1539-1554, 1995.
- Hitchman, M. H., and G. Brasseur, Rossby wave activity in a two-dimensional model: Closure for wave driving and meridional eddy diffusivity, *J. Geophys. Res.*, *93*, 9405-9417, 1988.
- Hitchman, M. H., M. A. McKay, and C. R. Trepte, A climatology of stratospheric sulfate aerosol, *J. Geophys. Res.*, *99*, 20689-20700, 1994.
- Holton, J. R., and J. Austin, The influence of the equatorial QBO on sudden stratospheric warmings, *J. Atmos. Sci.*, *48*, 607-618, 1991.
- Holton, J. R., and R. S. Lindzen, An updated theory for the quasi-biennial cycle of the tropical stratosphere, *J. Atmos. Sci.*, *29*, 1076-1080, 1972.
- Holton, J. R., and H. C. Tan, The influence of the equatorial quasi-biennial oscillation on the global circulation at 50 mb, *J. Atmos. Sci.*, *37*, 2200-2208, 1980.
- Huang, T. Y. W., The impact of solar radiation on the quasi-biennial oscillation of ozone in the tropical stratosphere, *Geophys. Res. Lett.*, *23*, 1135-1138, 1996.
- Kinnersley, J. S., and S. Pawson, The descent rates of the shear zones of the equatorial QBO, *J. Atmos. Sci.*, *53*, 1937-1949, 1996.
- Kodera, K., M. Chiba, and K. Shibata, A general circulation study of the solar and QBO modulation of the stratospheric circulation during the northern hemisphere winter, *Geophys. Res. Lett.*, *18*, 1209-1212, 1991.
- Lait, L. R., M. R. Schoberl, and P. A. Newman, Quasi-biennial modulation of the Antarctic ozone depletion, *J. Geophys. Res.*, *94*, 11559-11571, 1989.
- Li, D., K. P. Shine, and L. J. Gray, The role of ozone-induced diabatic heating anomalies in the quasi-biennial oscillation, *Q. J. R. Meteorol. Soc.*, *121*, 937-943, 1995.
- Lindzen, R. S., Turbulence and stress owing to gravity wave and tidal breakdown, *J. Geophys. Res.*, *86*, 9707-9714, 1981.
- Lindzen, R. S., and J. R. Holton, A theory of the quasi-biennial oscillation, *J. Atmos. Sci.*, *25*, 1095-1107, 1968.
- Ling, X.-D., and J. London, The quasi-biennial oscillation of ozone in the tropical middle stratosphere: A one-dimensional model, *J. Atmos. Sci.*, *43*, 3122-3137, 1986.
- Manzini, E., and K. Hamilton, Middle atmospheric traveling waves forced by latent and convective heating, *J. Atmos. Sci.*, *50*, 2180-2200, 1993.
- Naujokat, B., An update of the observed quasi-biennial oscillation of the stratospheric winds over the tropics, *J. Atmos. Sci.*, *43*, 1873-1877, 1986.
- Newman, P. A., Comparison of modeled and measured total column ozone, in *The Atmospheric Effect of Stratospheric Aircraft: Report of the 1992 Models and Measurements Workshop*, vol. II, *NASA Ref. Publ.* 1292, 1993.
- Oltmans, S. J., and J. London, The quasi-biennial oscillation in atmospheric ozone, *J. Geophys. Res.*, *87*, 8981-8989, 1982.
- O'Sullivan, D., and M. H. Hitchman, Inertial instability and Rossby wave breaking in a numerical model, *J. Atmos. Sci.*, *49*, 991-1002, 1992.
- O'Sullivan, D., and M. L. Salby, Coupling of the quasi-biennial oscillation and the extratropical circulation in the stratosphere through planetary wave transport, *J. Atmos. Sci.*, *47*, 650-673, 1990.
- Plumb, R. A., The interaction of two internal waves with

- the mean flow: Implications for the theory of the quasi-biennial oscillation, *J. Atmos. Sci.*, *34*, 1847-1858, 1977.
- Plumb, R. A., and R. C. Bell, Equatorial waves in a steady zonal shear flow, *Q. J. R. Meteorol. Soc.*, *108*, 313-334, 1982a.
- Plumb, R. A., and R. C. Bell, A model of the quasibiennial oscillation on an equatorial beta-plane, *Q. J. R. Meteorol. Soc.*, *108*, 335-352, 1982b.
- Plumb, R. A., and A. D. McEwan, The instability of a forced standing wave in a viscous stratified fluid: A laboratory analog of the quasi-biennial oscillation, *J. Atmos. Sci.*, *35*, 1827-1839, 1978.
- Randel, W. J., Global atmospheric circulation statistics, 1000 - 1 mb, *NCAR Tech. Note TN-295*, 245 pp., Nat. Cent. for Atmos. Res., Boulder, Colo., 1987.
- Reed, R. J., The present status of the 26-month oscillation, *Bull. Am. Meteorol. Soc.*, *46*, 374-387, 1965a.
- Reed, R. J., The quasi-biennial oscillation of the atmosphere between 30 and 50 km over Ascension Island, *J. Atmos. Sci.*, *22*, 331-333, 1965b.
- Reed, R. J., W. J. Campbell, L. A. Rasmussen, and D. G. Rogers, Evidence of a downward propagating annual wind reversal in the equatorial stratosphere, *J. Geophys. Res.*, *66*, 813-818, 1961.
- Shah, G. M., Quasi-biennial oscillation in ozone, *J. Atmos. Sci.*, *24*, 396-401, 1967.
- Stevens, D. E., H.-C. Kuo, W. H. Schubert, and P. E. Ciesielski, Quasi-balanced dynamics in the tropics, *J. Atmos. Sci.*, *47*, 2262-2273, 1990.
- Takahashi, M., and B. A. Boville, A three-dimensional simulation of the equatorial quasi-biennial oscillation, *J. Atmos. Sci.*, *49*, 1020-1035, 1992.
- Takahashi, M., and J. R. Holton, The mean zonal flow response to Rossby wave and gravity wave forcing in the equatorial lower stratosphere: Relationship to the QBO, *J. Atmos. Sci.*, *48*, 2078-2087, 1991.
- Takahashi, M., and M. Shiobara, A note on a QBO-like oscillation in a 1/5 sector three-dimensional model derived from a GCM, *J. Meteorol. Soc. Jpn.*, *73*, 131-137, 1995.
- Trepte, C. R., and M. H. Hitchman, Tropical stratospheric circulation deduced from satellite aerosol data, *Nature*, *335*, 626-628, 1992.
- Tung, K.-K., and H. Yang, Global QBO in circulation and ozone, I, Reexamination of observational evidence, *J. Atmos. Sci.*, *51*, 2699-2707, 1994a.
- Tung, K.-K., and H. Yang, Global QBO in circulation and ozone, II, A simple mechanistic model, *J. Atmos. Sci.*, *51*, 2708-2721, 1994b.
- van Loon, H., and K. Labitzke, The southern oscillation, V, The anomalies in the lower stratosphere of the northern hemisphere in winter and a comparison with the quasi-biennial oscillation, *Mon. Weather Rev.*, *115*, 357-369, 1987.
- Veryard, R. G., and R. A. Ebdon, Fluctuations in tropical stratospheric winds, *Meteorol. Mag.*, *90*, 125-143, 1961.
- Wallace, J. M., A note on the role of radiation in the biennial oscillation, *J. Atmos. Sci.*, *24*, 598-599, 1967a.
- Wallace, J. M., On the role of mean meridional motions in the biennial oscillation, *Q. J. R. Meteorol. Soc.*, *93*, 176-185, 1967b.
- Wallace, J. M., General circulation of the tropical lower stratosphere, *Rev. Geophys.*, *11*, 191-222, 1973.
- Wallace, J. M., R. L. Panetta, and J. Estberg, Representation of the equatorial stratospheric quasi-biennial oscillation in EOF phase space, *J. Atmos. Sci.*, *50*, 1751-1762, 1993.
- Xu, J.-S., On the relationship between the stratospheric quasi-biennial oscillation and the tropospheric southern oscillation, *J. Atmos. Sci.*, *49*, 725-734, 1992.
- Yao, C.-Y., Geographical variation of the annual and quasi-biennial cycles in the tropical lower stratosphere, M. S. thesis, 90 pp., Univ. of Wis. - Madison, 1994.
- Yasunari, T., A possible link of the QBOs between the stratosphere, troposphere and sea surface temperature in the tropics, *J. Meteorol. Soc. Jpn.*, *67*, 483-493, 1989.
- Zawodny, J. M., and M. P. McCormick, Stratospheric aerosol and gas experiment II measurements of the quasi-biennial oscillations in ozone and nitrogen dioxide, *J. Geophys. Res.*, *96*, 9371-9377, 1991.
- Zerefos, C. S., A. F. Bais, I. C. Ziomas, and R. D. Bojkov, On the relative importance of the quasi-biennial oscillation and El Nino/southern oscillation in the revised Dobson total ozone records, *J. Geophys. Res.*, *97*, 10135-10144, 1992.

---

P. A. Politowicz and M. H. Hitchman, Department of Atmospheric and Oceanic Sciences, University of Wisconsin - Madison, 1225 W. Dayton Street, Madison, WI 53706. (e-mail: philp@ssc.wisc.edu; matt@adams.meteor.wisc.edu)

(Received December 28, 1994; revised February 21, 1997; accepted February 24, 1997.)